

CUTTING PATTERN DESIGN OF MEMBRANE STRUCTURES CONSIDERING VISCOELASTICITY OF MATERIAL

J. Fujiwara¹⁾, M. Ohsaki¹⁾ and K. Uetani¹⁾

1) Department of Architecture and Architectural Systems,
Kyoto University, Sakyo, Kyoto 606-8501, Japan

ABSTRACT

A method is presented for determination of cutting patterns of membrane structures considering viscoelasticity of material. A constitutive law is proposed to represent viscoelastic behavior of material in the range around the target stress level. By using the proposed constitutive law, relaxation behavior of a membrane structure is estimated without time-history analysis, and the initial stress immediately after construction is determined to obtain stresses close to the target value at the steady state when relaxation is terminated. The effectiveness of the proposed method is discussed in the example.

1. INTRODUCTION

In the construction process of a membrane structure, the curved surface is formed by stretching pieces of plane cutting sheets and connecting them to a frame. However, because of viscosity of material, prestresses are reduced after construction and equilibrium shape deforms due to well-known phenomenon called relaxation. As prestresses are given so that the surface retains stability and stiffness against external loads, deformation due to external loads may increase after relaxation.

Minami *et al.*¹ developed an experimental method for finding the stress-strain relation after relaxation. They determined bi-axial stress-strain curves based on the results of experiments and proposed a method for relaxation analysis using the obtained stress-strain curves. Kato *et al.*² proposed a visco-elastoplastic constitutive law based on a fabric lattice model and carried out relaxation analysis considering the construction process. The constitutive law, however, has many parameters to be determined.

Tsubota and Yoshida³ optimized cutting patterns by repeating the process of shape analysis and modification of cutting patterns. Ohsaki *et al.*⁴⁻⁶ proposed a method for optimizing equilibrium shape and stresses under the condition that equilibrium shape is reduced to plane sheets after releasing the stresses. Uetani *et al.*⁷ determined optimal

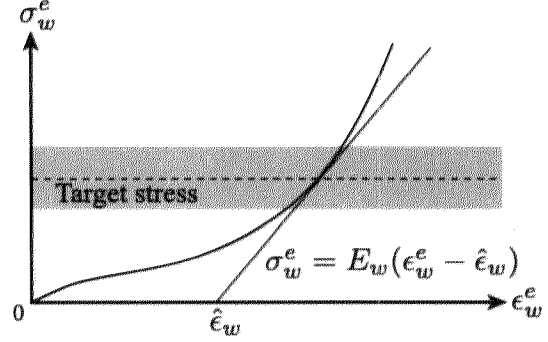
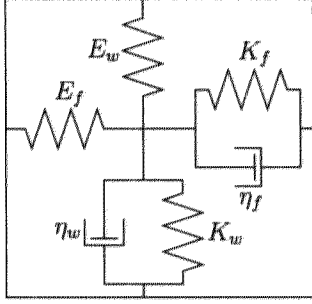


Fig. 1: An orthotropic 3-parameter model. Fig. 2: Approximate stress-strain relation.

equilibrium shape and cutting patterns simultaneously by solving linearized forms of equilibrium equations and optimality conditions. In these methods, however, the membrane is modeled as an orthotropic elastic material, and viscosity is not considered.

In this paper, a constitutive law is proposed for representing viscoelastic behavior of material in the range around the target stress level. The material parameters are obtained from bi-axial tests of membrane sheets. The elastic stress-strain relation is then obtained from the proposed constitutive law at the steady state when relaxation behavior is terminated. A cutting pattern optimization method is also presented for minimizing the stress deviation at the steady state.

2. CONSTITUTIVE LAW OF MEMBRANE MATERIAL

In this section, a viscoelastic law of the membrane is proposed for modeling the material properties. We propose the model as shown in Fig. 1 which is the simplest model that can represent the elastic and viscoelastic behavior. In the following, the part of parallel connected dashpot and spring is called *viscous part*, and the remaining spring is called *elastic part*. Let $()^e$ and $()^v$ denote the values corresponding to the elastic and viscous parts, respectively.

The stress and strain in warp direction are denoted by σ_w and ϵ_w , respectively. The elastic modulus of elastic part, that of viscous part and viscous modulus are denoted by E_w , K_w and η_w , respectively, as shown in Fig. 1. In fill (weft) direction, σ_f , ϵ_f , E_f , K_f and η_f are defined similarly. The shear stress, shear strain and shear modulus are denoted by τ_{wf} , γ_{wf} and E_{wf} , respectively.

2.1 Elastic law of the membrane

The elastic law is derived by restricting deformations of the dashpots of the model in Fig. 1. Although stress-strain relation of the membrane is generally modeled by a nonlinear curve as shown in Fig. 2, the membrane is modeled here as a linear orthotropic material⁶. The linearized relation and Poisson's ratio are determined for approximating stress-strain relations in the range around the target stress as shown in Fig. 2.

It is assumed that elastic deformations in the warp and fill directions influence each other through Poisson's ratio. Let $\hat{\epsilon}_w$ be defined as shown in Fig. 2. $\hat{\epsilon}_f$ is given similarly.

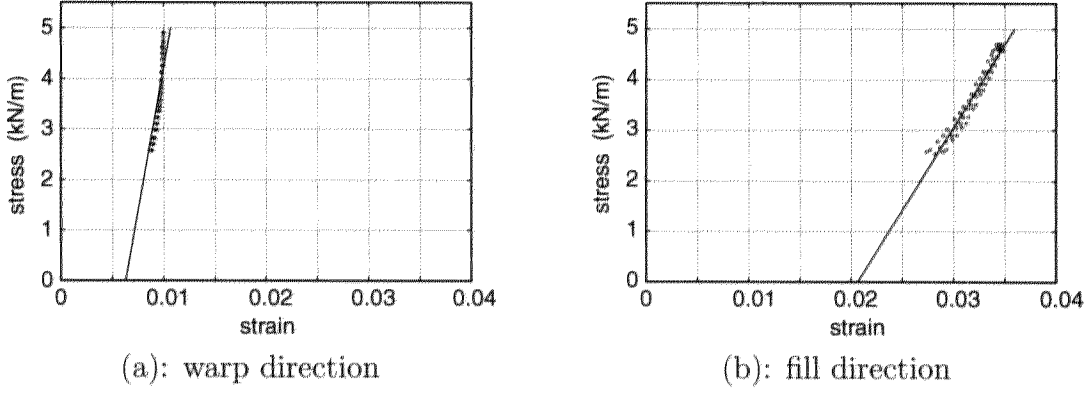


Fig. 3: Elastic stress-strain relations.

The stress-strain relations under bi-axial loading are written as

$$\epsilon_w^e = \frac{1}{E_w} \sigma_w^e - \frac{\nu_f}{E_f} \sigma_f^e + \bar{\epsilon}_w, \quad \epsilon_f^e = \frac{1}{E_f} \sigma_f^e - \frac{\nu_w}{E_w} \sigma_w^e + \bar{\epsilon}_f \quad (1)$$

where ν_f and ν_w are Poisson's ratios, $\bar{\epsilon}_w = \hat{\epsilon}_w - \nu_f \hat{\epsilon}_f$ and $\bar{\epsilon}_f = \hat{\epsilon}_f - \nu_w \hat{\epsilon}_w$. τ_{wf} is assumed to be proportional to τ_{wff} as

$$\tau_{wf} = E_{wf} \gamma_{wf} \quad (2)$$

Relation between the stress vector $\boldsymbol{\sigma}^e = \{\sigma_w^e, \sigma_f^e, \tau_{wf}\}^T$ of elastic part and the strain vector $\boldsymbol{\epsilon}^e = \{\epsilon_w^e, \epsilon_f^e, \gamma_{wf}\}^T$ of elastic part is derived from (1) and (2) as

$$\boldsymbol{\sigma}^e = \mathbf{D}(\boldsymbol{\epsilon}^e - \bar{\boldsymbol{\epsilon}}) \quad (3)$$

where $\bar{\boldsymbol{\epsilon}} = \{\bar{\epsilon}_w, \bar{\epsilon}_f, 0\}^T$ and \mathbf{D} is the constitutive matrix determined from (1) and (2).

E_w , E_f , ν_f and ν_w are to be obtained from the bi-axial cyclic loading test⁸. $\hat{\epsilon}_w$ and $\hat{\epsilon}_f$ are determined so as to minimize the sum of squares of errors between the test results and the values calculated from (3). The test results have been obtained from the case where the ratio between the warp stress and the fill stress, which is simply called *stress ratio*, is 1 : 1. Only the data for the stress range 2.50 - 5.00 kN/m in the third, fourth and fifth loading process have been used.

The stress-strain relations are as shown in Figs. 3 (a), (b), where dots are experimental results, and solid lines are the results by (3). It may be observed from Figs. 3 (a), (b) that the proposed elastic law can represent the elastic stress-strain relation within good accuracy in the target stress range (2.50 - 5.00 kN/m).

2.2 Viscoelastic law of the membrane

Let $(\dot{})$ denote differentiation with respect to time. By differentiating (1) with respect to time and by setting $\dot{\hat{\epsilon}}_w = \dot{\hat{\epsilon}}_f = 0$, $\dot{\epsilon}_w^e$ is derived as

$$\dot{\epsilon}_w^e = \frac{1}{E_w} \dot{\sigma}_w^e - \frac{\nu_f}{E_f} \dot{\sigma}_f^e \quad (4)$$

Because a spring and a dashpot are connected in parallel in the viscous part, the warp stress σ_w^v is represented as the sum of stresses of the spring and dashpot. Since the deformations in warp and fill directions are assumed to be independent at the viscous part, the following equation is derived:

$$\sigma_w^v = K_w \epsilon_w^v + \eta_w \dot{\epsilon}_w^v \quad (5)$$

Because the total strain ϵ_w in warp direction is the sum of ϵ_w^e and ϵ_w^v ($\epsilon_w = \epsilon_w^e + \epsilon_w^v$), (5) is rewritten from (1) as

$$\begin{aligned} \dot{\epsilon}_w^v &= \frac{1}{\eta_w} \sigma_w^v - \frac{K_w}{\eta_w} (\epsilon_w - \epsilon_w^e) \\ &= \frac{1}{\eta_w} \sigma_w^v - \frac{K_w}{\eta_w} \left\{ \epsilon_w - \left(\frac{1}{E_w} \sigma_w^e - \frac{\nu_f}{E_f} \sigma_f^e + \bar{\epsilon}_w \right) \right\} \end{aligned} \quad (6)$$

From $\epsilon_w = \epsilon_w^e + \epsilon_w^v$, the total strain velocity $\dot{\epsilon}_w$ in warp direction is given as the sum of $\dot{\epsilon}_w^e$ and $\dot{\epsilon}_w^v$. Since the elastic part and viscous part are connected serially, $\sigma_w^e = \sigma_w^v = \sigma_w$. Hence, the following relation is derived from (4) and (6)

$$\dot{\epsilon}_w = \frac{1}{\eta_w} \frac{E_w + K_w}{E_w} \sigma_w - \frac{\nu_f K_w}{\eta_w E_f} \sigma_f + \frac{1}{E_w} \dot{\sigma}_w^e - \frac{\nu_f}{E_f} \dot{\sigma}_f^e - \frac{K_w}{\eta_w} (\epsilon_w - \bar{\epsilon}_w) \quad (7)$$

$\dot{\epsilon}_f$ is given similarly. Since viscosity is not considered in the shear deformation, the relation between $\dot{\tau}_{wf}$ and $\dot{\gamma}_{wf}$ is written from (2) as

$$\dot{\tau}_{wf} = E_{wf} \dot{\gamma}_{wf} \quad (8)$$

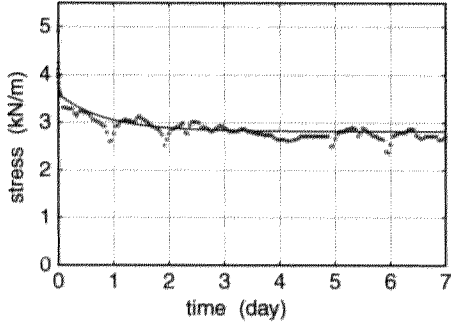
Eqns. (7) and (8) are rewritten simply by using the stress vector $\boldsymbol{\sigma} = \{\sigma_w, \sigma_f, \tau_{wf}\}^T$ and the strain vector $\boldsymbol{\epsilon} = \{\epsilon_w, \epsilon_f, \gamma_{wf}\}^T$ as

$$\mathbf{G}\boldsymbol{\sigma} + \mathbf{D}^{-1}\dot{\boldsymbol{\sigma}} = \mathbf{H}(\boldsymbol{\epsilon} - \bar{\boldsymbol{\epsilon}}) + \dot{\boldsymbol{\epsilon}} \quad (9)$$

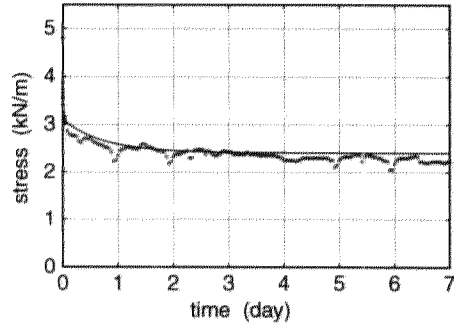
where \mathbf{G} and \mathbf{H} are the constitutive matrix obtained from (7) and (8).

In the following, material parameters in (9) are obtained from bi-axial relaxation test which has been carried out in Ref. 8. Because E_w , E_f , ν_f and ν_w are already given, only K_w , η_w , K_f and η_f should be determined here. Material parameters are defined so as to minimize the sum of squares of errors of the stresses calculated by time-history analysis from the test results. Due to loosening of the yarn, a rapid relaxation is usually observed immediately after stretching the membrane. In a practical situation, however, the membrane sheets are pre-stretched to remove the looseness of yarn. Hence, the deformation within an hour after loading is neglected. The time-history analysis begins after an hour from loading and the stress at the time is regarded as the initial stress of the analysis. Since the strain is fixed in the relaxation test, the strain is calculated from (3) and the initial stress by letting $\dot{\epsilon}_w = \dot{\epsilon}_f = 0$. The increment of time is 0.5 hour.

The material parameters that minimize the error are obtained by the quasi-Newton method. The sensitivity coefficients is calculated by the finite difference method. The



(a): 1 : 1, warp direction



(b): 1 : 1, fill direction

Fig. 4: Results by relaxation tests and analyses.

results by experiment and analysis using the parameters estimated from the data of 1 : 1, 2 : 1 and 1 : 2 are as shown in dots and solid curves, respectively, in Figs. 4 (a), (b). It is observed from Figs. 4 (a), (b) that the proposed viscoelastic law can represent relaxation behavior within good accuracy. It has been confirmed that the errors of stresses for the stress ratios 2 : 1 and 1 : 2 are sufficiently small, even if the parameters are estimated from the data of only 1 : 1.

3. CUTTING PATTERN DESIGN

A method for cutting pattern design is presented to obtain stresses close to the target values at the steady state when relaxation is terminated. Reduction of stresses due to relaxation is estimated by using the proposed constitutive equations, and the target stress immediately after construction, which is simply called as the *initial target stress*, is determined so as to realize the stresses at the steady state close to the target values.

The stress-strain relation at the steady state is derived by removing the dashpots from the model of Fig. 1, because the stress velocity vanishes. Therefore, relation between σ and ϵ at the steady state is written as

$$\epsilon - \bar{\epsilon} = D_t^{-1} \sigma \quad (10)$$

where D_t is the constitutive matrix obtained from (2), (9) and $\dot{\sigma} = \dot{\epsilon} = 0$

If the membrane structure is discretized by triangular finite elements with uniform stresses, the initial target stress is determined by the following process:

- D1** Specify the boundary shape and the target stress vector $\bar{\sigma}$ of all the elements at the steady state.
- D2** Carry out equilibrium shape analysis and find the nodal coordinates of all the nodes on the equilibrium surface satisfying $\sigma = \bar{\sigma}$.
- D3** Calculate strain vector $\tilde{\epsilon}$ of all the elements by using (10); i.e. $\tilde{\epsilon} = \bar{\epsilon} + D_t^{-1} \bar{\sigma}$.
- D4** Remove the deformation corresponding to $\tilde{\epsilon}$ from the triangular elements on the equilibrium surface and find the unstressed triangles that do not satisfy compatibility conditions between the elements.

D5 Connect the unstressed triangles and carry out nonlinear elastic analysis by stretching them to the boundary to find the stress vector $\hat{\sigma}$ of all the elements which are taken as the initial target stresses for cutting pattern design.

In the proposed method, it is not necessary to carry out time history analysis, because the stress-strain relation at the steady state is simply given as (10). Moreover, the changes of equilibrium shape due to relaxation is incorporated. Hence, if stresses immediately after construction are equal to $\hat{\sigma}$, stresses after relaxation converge to $\bar{\sigma}$.

Note that the proposed method does not depend on method for the cutting pattern design. The target stress, however, should be in the range where accuracy of the constitutive law is guaranteed.

4. EXAMPLE

Consider a frame-supported membrane as shown in Figs. 5 (a), (b), where the boundary nodes b, c, d and e make a square with $W = 9.0$ m, and the height of the triangle abe with $\overline{ab} = \overline{ae}$ is 1.2 m. In Fig. 5 (b), solid lines are boundary beams, and dotted curves are cutting curves. Material properties are as listed in Table 1.

The target values (kN/m) for σ_w , σ_f and τ_{wf} at steady state are 3.0, 3.0 and 0.0, respectively. The method in Ref. 6 is used for cutting pattern design. Considering symmetry of the membrane, cutting pattern design and relaxation analysis are carried out for only a half of the surface. Two cases of the initial target stresses are considered. In Case A, $\hat{\sigma}$ is determined by the algorithm proposed in the previous section. In Case B, the target stress at steady state is directly given for $\hat{\sigma}$.

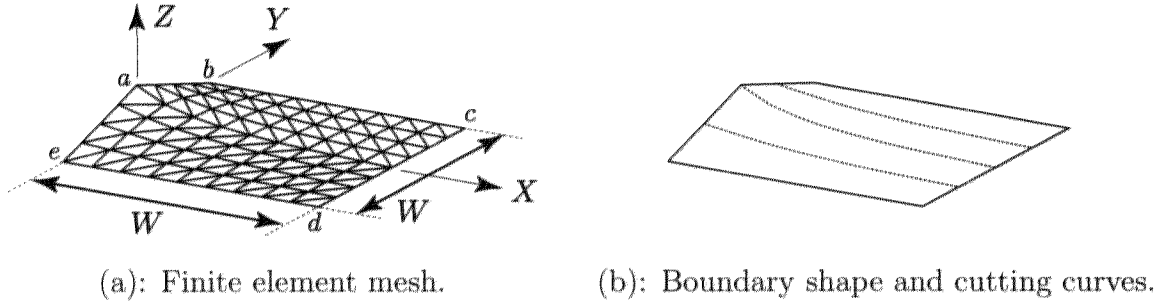
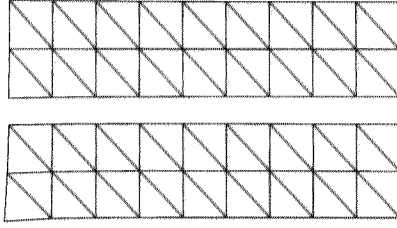


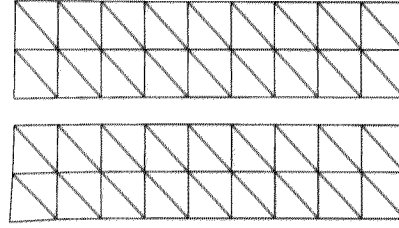
Fig. 5: A frame-supported membrane.

Table 1: Material properties.

E_w	9.92×10^2 kN/m	E_f	3.13×10^2 kN/m
ν_f	4.20×10^{-2}	ν_w	1.30×10^{-1}
$\hat{\epsilon}_w$	7.22×10^{-3}	$\hat{\epsilon}_f$	2.16×10^{-2}
K_w	4.31×10^3 kN/m	K_f	1.21×10^3 kN/m
η_w	4.66×10^3 kN · day/m	η_f	1.14×10^3 kN · day/m
E_{wf}	1.65×10^2 kN/m		



(a): Case A



(b): Case B

Fig. 6: Cutting patterns.

Table 2: Results of relaxation analysis.

(a): Immediately after construction.

	Case A			Case B		
Stress deviation $((\text{kN/m})^2)$	175.053			17.489		
Stress (kN/m)	σ_w	σ_f	τ_{wf}	σ_w	σ_f	τ_{wf}
Target value	3.000	3.000	0.000	3.000	3.000	0.000
Mean value	4.004	4.130	0.025	3.172	3.266	0.025
Maximum value	4.461	5.123	0.886	3.622	4.240	0.870
Minimum value	3.430	3.840	-0.768	2.609	2.982	-0.759
Standard deviation	0.267	0.169	0.216	0.264	0.167	0.212

(b): After 10 days from construction.

	Case A			Case B		
Stress deviation $((\text{kN/m})^2)$	14.616			39.663		
Stress (kN/m)	σ_w	σ_f	τ_{wf}	σ_w	σ_f	τ_{wf}
Target value	3.000	3.000	0.000	3.000	3.000	0.000
Mean value	3.151	3.251	0.024	2.497	2.571	0.023
Maximum value	3.555	4.043	0.866	2.895	3.348	0.847
Minimum value	2.655	3.004	-0.736	2.011	2.329	-0.725
Standard deviation	0.234	0.136	0.207	0.231	0.134	0.204

After obtaining the cutting patterns, elastic analysis and relaxation analysis are to be carried out. Relaxation analysis is terminated after 10 days from construction when relaxation behavior of the membrane can be assumed to be almost stationary.

Figs. 6 (a), (b) show the obtained cutting patterns for Cases A and B. The results of relaxation analysis are as shown in Tables 2 (a), (b), where stress deviation is the sum of squares of errors from the target stress. It is observed from Table 2 (a) that the stress deviation is small for Case B immediately after construction. The stresses at steady state for Case B, however, are about 80 % of the target values due to relaxation. On the other hand, stresses for Case A are sufficiently close to the target values at the steady state.

It may be observed from these results that the cutting patterns can be successfully generated by using proposed method to obtain stresses close to the target values at the steady state.

5. CONCLUSIONS

A constitutive law for the membrane has been proposed based on a 3-parameter orthotropic model. Although the number of material parameters is small, the proposed constitutive law has good accuracy in the target range of stresses. By comparing numerical and experimental results, it has been shown that the proposed constitutive law can accurately represent the elastic and viscoelastic behaviors.

The stress-strain relation at the steady state has been derived from the proposed constitutive law by removing the dashpots. By using the derived relation, equilibrium shape and stresses at steady state can easily be found without time-history analysis. A method has also been presented for determining the initial target stresses for cutting pattern design so as to minimize the stress deviation at the steady state.

In the example, the proposed method has been applied to a frame-supported membrane structure modeled by the triangular finite elements with uniform stresses. It has been shown that the cutting patterns are easily found for realizing stresses at the steady state close to the target values.

REFERENCES

1. H. Minami, C. Yamamoto, S. Segawa and Y. Kono: Bi-axial stress-strain curves for nonlinear analysis of membrane considering the effect of stress relaxation or creep, *Proc. of the IASS 40th anniversary congress*, Madrid, 1999, Vol.1, pp.C1.73-C1.81
2. S. Kato, T. Yoshino, H. Minami and S. Segawa: Study on the construction process of membrane structures considering visco-elast-plastic analysis, *Proc. of the IASS 40th anniversary congress*, Madrid, 1999, Vol.1, pp.C1.93-C1.102
3. H. Tsubota and A. Yoshida: Theoretical analysis for determining optimum cutting patterns for membrane structures, *Proc. of IASS Symposium on 10 Years of Progress in Shell and Spatial Structures*, Vol.3, Madrid, Spain, 1989.
4. M. Ohsaki, K. Uetani and S. Takatani: Shape-stress trade-off design method of membrane structures by using inverse problem approach, *J. Struct. Constr. Eng., AIJ*, No.488, pp.107-115, 1996. (Japanese)
5. M. Ohsaki and K. Uetani: Shape-stress trade-off design method of membrane structures for specified sequence of boundary shapes, *Comput. Method Appl. Mech. Engrg.*, 182, pp.73-88, 2000.
6. M. Ohsaki and J. Fujiwara: Shape and stress optimization of membrane structures considering material nonlinearity, *Research Report on Membrane Structures '98*, No.12, pp.1-8, 1998. (in Japanese)
7. K. Uetani, E. Mitsuda and M. Ohsaki: Cutting-pattern optimization of membrane structures by parametric approach with respect to boundary shape, *Proc. IASS-IACM 2000*, 2000.
8. E. Fujii: Determination of initial stress field and optimal pretensioning of a frame-supported membrane, Master's thesis, Dept. of Architecture and Architectural Systems, Kyoto University, 1997. (in Japanese)
9. J. S. Arora and C. H. Tseng: IDESIGN User's Manual Ver. 3.5. Optimal Design Laboratory, University of Iowa, Iowa City, Iowa., 1987.